

On the Behavior of the Distributed Coordination Function of IEEE 802.11 with Multirate Capability under General Transmission Conditions

F. Daneshgaran, M. Laddomada, F. Mesiti, and M. Mondin

Abstract—The aim of this paper is threefold. First, it presents a multi-dimensional Markovian state transition model characterizing the behavior of the IEEE 802.11 protocol at the Medium Access Control layer which accounts for packet transmission failures due to channel errors modeling both saturated and non-saturated traffic conditions. Second, it provides a throughput analysis of the IEEE 802.11 protocol at the data link layer in both saturated and non-saturated traffic conditions taking into account the impact of both the physical propagation channel and multirate transmission in Rayleigh fading environment. The general traffic model assumed is M/M/1/K. Finally, it shows that the behavior of the throughput in non-saturated traffic conditions is a linear combination of two system parameters; the payload size and the packet rates, $\lambda^{(s)}$, of each contending station. The validity interval of the proposed model is also derived.

Simulation results closely match the theoretical derivations, confirming the effectiveness of the proposed models.

Index Terms—DCF, Distributed Coordination Function, fading, IEEE 802.11, MAC, Rayleigh fading, rate adaptation, saturation, throughput, unsaturated, non-saturated.

I. INTRODUCTION

The IEEE802.11 Medium Access Control (MAC) layer [1] presents a mandatory option, namely the Distributed Coordination Function (DCF), based on the Carrier Sense Multiple Access Collision Avoidance CSMA/CA access method, that has received considerable attention in the past years [3]-[18].

Many papers, following the seminal work by Bianchi [3], have addressed the problem of modeling the DCF in a variety of traffic load and channel transmission conditions. Most of them focus on a scenario presenting N saturated stations that transmit towards a common Access Point (AP) under the hypotheses that the packet rates, along with the probability of transmission in a randomly chosen time slot, is common to all the involved stations, while the error events on the transmitted packets are mainly due to collisions between packets belonging to different stations.

Real networks are different in many respects. First, traffic is mostly non-saturated, so it is important to derive a model accounting for practical network operations. Channel conditions are far from being ideal and often packet transmission has to be rescheduled until data is correctly received. Due to Rayleigh and shadow fading conditions, a real scenario

This work has been supported by Euroconcepts, S.r.l. (<http://www.euroconcepts.it>)

F. Daneshgaran is with ECE Dept., California State University, Los Angeles, USA.

M. Laddomada, F. Mesiti, and M. Mondin are with DELEN, Politecnico di Torino, Italy.

presents stations transmitting at different bit rates, because of multirate adaptation foreseen at the physical layer of WLAN protocols such as IEEE 802.11b. Furthermore, other scenarios usually occur in a real network. As an example, different stations usually operate with different loads, i.e., they have different packet rates, while the transmitting bit rate can also differ between the contending stations. In all these situations the common hypothesis, widely employed in the literature, that all the contending stations have the same probability of transmitting in a randomly chosen time slot, does not hold anymore. The aim of this paper is to provide a model and theoretical analysis under much more realistic scenarios. With this background, let us provide a quick survey of the recent literature related to the problem addressed in this paper.

In [3], the author provides an analysis of the saturation throughput of the basic 802.11 protocol assuming a two dimensional Markov model at the MAC layer. Papers [4]-[6] model the influence of real channel conditions on the throughput of the DCF operating in saturated traffic conditions, while [7]-[9] thoroughly analyze the influence of capture on the throughput of wireless transmission systems.

The behavior of the DCF of IEEE 802.11 WLANs in unsaturated traffic conditions has been analyzed in a number of papers [10]-[12]. In [10] the authors extend the Bianchi's model by introducing a new state in order to consider non-saturated traffic conditions, accounting for the case in which the station queue is empty after successful completion of a packet transmission. In the modified model however, a packet is discarded after m backoff stages, while in Bianchi's model the station keeps iterating in the m -th backoff stage until the packet gets successfully transmitted. These models rely on the basic hypotheses of ideal channel transmission and on the absence of capture effects. Paper [11] proposes to model non-saturated traffic conditions by adding a new state for each backoff stage accounting for the absence of new packets to be transmitted. In [12]-[13], the authors extend the multi-dimensional Markovian state transition model characterizing the MAC layer behavior by including transmission states that account for packet transmission failures due to errors caused by propagation through the channel, along with a state characterizing the situation when a station has no packets to transmit.

In [14], the authors look at the impact of channel induced errors and of the received SNR on the achievable throughput in a system with rate adaptation, whereby the transmission rate of the terminal is modified depending on either direct

or indirect measurements of the link quality. In [15], the authors were the first to observe that in multirate networks the aggregate throughput is strongly influenced by that of the slowest contending station; such a phenomenon is denoted as “performance anomaly of the DCF of IEEE 802.11 protocol”. In [16], authors provide an analytical framework for analyzing the link delay of multirate networks. In [18], authors provide DCF models for finite load sources with multirate capabilities, while in [17] authors propose a DCF model for networks with multirate stations and derive the saturation throughput. Remedies to performance anomalies are also discussed. In both previous works, packet errors are only due to collisions between different contending stations.

In this paper, we substantially extend the previous work proposed in the companion papers [12]-[13] by looking at all the three issues outlined before together, namely, real channel conditions, saturated and non-saturated traffic, and multirate capabilities. Our basic assumptions are essentially similar to those of Bianchi [3], with the exception that we do assume the presence of both channel induced errors due to the transmission over Rayleigh fading channel, and we consider a general traffic model. As a reference standard, we use network parameters belonging to the IEEE802.11b protocol, even though the proposed mathematical model holds for any flavor of the IEEE802.11 family or other wireless protocols with similar MAC layer functionality. We also derive a simple model of the aggregate throughput in unloaded traffic conditions and show that essentially, the throughput depends on the linear combination of the packet rates $\lambda^{(s)}$ of each contending station, each properly weighted by its payload size, while packet errors due to imperfect channel conditions do not affect the aggregate throughput. The validity interval of the proposed model is also derived.

The paper is organized as follows. After a brief review of the functionalities of the contention window procedure at MAC layer, Section II substantially extends the Markov model initially proposed by Bianchi, presenting modifications that account for transmission errors over Rayleigh fading channels employing the 2-way handshaking technique in a variety of traffic conditions. Section III is devoted to the solution of the proposed bi-dimensional Markov chain related to each contending station, and provides an expression for the aggregate throughput of the link. After defining the basic time parameters needed for system performance evaluation, Section IV estimates the expected time slot duration needed for the evaluation of the aggregate throughput of the link. The adopted traffic model is discussed in Section V.

Section VI briefly addresses the modeling of the physical layer of IEEE 802.11b in a variety of channel conditions. In Section VII we present simulation results where typical MAC layer parameters for IEEE802.11b are used to obtain throughput values as a function of various system level parameters and SNR, under typical traffic conditions. Section VIII derives a simple model of the aggregate throughput in unsaturated traffic conditions, along with its interval of validity. Insights on the DCF behavior with multiple contending stations are also given, considering a multirate setting. Finally, Section IX is devoted to conclusions.

II. MARKOVIAN MODEL CHARACTERIZING THE MAC LAYER UNDER GENERAL TRAFFIC CONDITIONS AND REAL TRANSMISSION CHANNEL

In a previous paper [12], we proposed a bi-dimensional Markov model for characterizing the behavior of the DCF under a variety of real traffic conditions, both non-saturated and saturated, with packet queues of small sizes, and considered the IEEE 802.11b protocol with the basic 2-way handshaking mechanism. Many of the basic hypotheses were the same as those adopted by Bianchi in the seminal paper [3].

As a starting point for the derivations which follow, we adopt the bi-dimensional model proposed in the companion paper [12], appropriately modified in order to account for a scenario of N contending stations, each one employing a specific bit rate and a different transmission packet rate. As in [12], we consider the IEEE 802.11b protocol employing the basic 2-way handshaking mechanism. For conciseness, we refer the interested to [12] for many details on the considered bi-dimensional Markov model.

Consider the following scenario: N stations transmit towards a common AP in infrastructure mode, whereby each station, characterized by its own traffic load, can access the channel using a data rate in the set $\{1, 2, 5.5, 11\}$ Mbps, depending on channel conditions. Each bit rate is associated with a different modulation format, whereas the basic rate is 1 Mbps with DBPSK modulation (2Mbps with DQPSK if short preamble is used) [1]. We identify a generic station with the index $s \in S = \{1, 2, \dots, N\}$, where N is the number of stations in the network, and S is the set of station indexes. As far as the transmission data rate is concerned, we define four rate-classes identified by a *rate-class identifier* r taking values in the set $R = \{1, 2, 3, 4\}$ ordered by increasing values of data rates $R_D = \{1, 2, 5.5, 11\}$ Mbps (as an example, rate-class $r = 3$ is related to the bit rate 5.5 Mbps). Concerning control packets and PLCP header transmissions, the basic rate is identified by R_C . Two basic rates are available for control packets, namely 1 and 2 Mbps, whereby the latter is adopted for short preambles [1].

The traffic load of the s -th station is identified by a Packet Arrival Rate (PAR) $\lambda^{(s)}$. Upon defining both rate-classes and traffic, we can associate a generic station s to a rate-class $r \in R$ and traffic load $\lambda^{(s)}$. As a consequence, with respect to the model in [12], we need to specify the probabilities along with different Markov chains for each station in the network.

The two sources of errors on the transmitted packets are collisions between packets and channel induced errors. Considering the s -th station, collisions can occur with probability $P_{col}^{(s)}$, while transmission errors due to imperfect channel transmissions can occur with probability $P_e^{(s)}$. Notice that $P_e^{(s)}$ depends upon the station rate-class r , which in turn depends on the Signal-to-Noise Ratio (SNR) received by the AP (appropriate expressions will be provided in Section VI for each rate-class). We assume that collisions and transmission error events are statistically independent. In this scenario, a packet from the s -th station is successfully transmitted if there is no collision (this event has probability $1 - P_{col}^{(s)}$) and the packet encounters no channel errors during transmission (this

For future developments, from the model depicted in Fig. 1 we note the following relations:

$$\begin{aligned} b_{i,0} &= P_{eq} \cdot b_{i-1,0} = P_{eq}^i \cdot b_{0,0}, \quad \forall i \in [1, m-1] \\ b_{m,0} &= \frac{P_{eq}^m}{1-P_{eq}} \cdot b_{0,0}, \quad i = m \end{aligned} \quad (3)$$

whereby, P_{eq} is the equivalent probability of failed transmission² that takes into account the need for a new contention due to either packet collision (P_{col}) or channel errors (P_e).

Let us focus on the meaning of the idle state I noted in Fig. 1 to which the stationary probability b_I is associated. This state considers both the situation in which after a successful transmission there are no packets in the station queue to be transmitted, and the situation in which the packet queue is empty and the station is waiting for new packet arrivals. The stationary probability of being in state b_I can be evaluated as follows:

$$\begin{aligned} b_I &= (1-q)(1-P_{eq}) \sum_{i=0}^m b_{i,0} + (1-P_{I,0})b_I \\ &= \frac{(1-q)(1-P_{eq})}{P_{I,0}} \cdot \sum_{i=0}^m b_{i,0} \end{aligned} \quad (4)$$

Upon employing the probabilities $b_{i,0}$ noted in (3), it is straightforward to obtain:

$$\sum_{i=0}^m b_{i,0} = b_{0,0} \left[\sum_{i=0}^{m-1} P_{eq}^i + \frac{P_{eq}^m}{1-P_{eq}} \right] = \frac{b_{0,0}}{1-P_{eq}} \quad (5)$$

By using the previous result, (4) simplifies to

$$b_I = \frac{1-q}{P_{I,0}} \cdot b_{0,0} \quad (6)$$

Equ. (4) reflects the fact that state b_I can be reached after a successful packet transmission from any state $b_{i,0}$, $\forall i \in [0, m]$ with probability $(1-q)(1-P_{eq})$, or because the station remains in idle state with probability $(1-P_{I,0})$, whereby $P_{I,0}$ is the probability of having at least one packet to be transmitted in the queue. The statistical model of $P_{I,0}$ will be discussed in Section V. It is anticipated that $P_{I,0}$ is related to the specific traffic model chosen for modeling packet arrivals in the station queue.

The other stationary probabilities for any $k \in [1, W_i - 1]$ follow by resorting to the state transition diagram shown in Fig. 1:

$$b_{i,k} = \frac{W_i - k}{W_i} \begin{cases} q(1-P_{eq}) \cdot \sum_{i=0}^m b_{i,0} + \\ + P_{I,0} \cdot b_I, & i = 0 \\ P_{eq} \cdot b_{i-1,0}, & i \in [1, m-1] \\ P_{eq}(b_{m-1,0} + b_{m,0}), & i = m \end{cases} \quad (7)$$

Upon substituting (4) in (7), $b_{0,k}$ can be obtained as follows:

$$\begin{aligned} q(1-P_{eq}) \cdot \sum_{i=0}^m b_{i,0} + P_{I,0} \cdot b_I &= \\ q(1-P_{eq}) \cdot \sum_{i=0}^m b_{i,0} + P_{I,0} \cdot \frac{(1-q)(1-P_{eq})}{P_{I,0}} \cdot \sum_{i=0}^m b_{i,0} &= \\ = (1-P_{eq}) \cdot \sum_{i=0}^m b_{i,0} \end{aligned} \quad (8)$$

²For simplicity, we assume that at each transmission attempt, any station will encounter a constant and independent probability of failed transmission, P_{eq} , independently from the number of retransmissions already suffered by each station.

Employing the normalization condition, after some mathematical manipulations, and remembering (5), it is possible to obtain:

$$\begin{aligned} 1 &= \sum_{i=0}^m \sum_{k=0}^{W_i-1} b_{i,k} + b_I \\ &= \frac{b_{0,0}}{2} \left\{ W_0 \left[\sum_{i=0}^{m-1} (2P_{eq})^i + \frac{(2P_{eq})^m}{1-P_{eq}} \right] + \frac{1}{1-P_{eq}} \right\} + b_I \\ &= \alpha \cdot b_{0,0} + b_I \end{aligned} \quad (9)$$

whereby,

$$\alpha = \frac{1}{2} \left\{ W_0 \left[\frac{1-(2P_{eq})^m}{1-2P_{eq}} + \frac{(2P_{eq})^m}{1-P_{eq}} \right] + \frac{1}{1-P_{eq}} \right\} \quad (10)$$

From (9), the following equation for computation of $b_{0,0}$ easily follows:

$$b_{0,0} = \frac{1-b_I}{\alpha} \quad (11)$$

Equ. (11) is used to compute $\tau^{(s)}$, the probability that the s -th station starts a transmission in a randomly chosen time slot. In fact, taking into account that a packet transmission occurs when the backoff counter reaches zero, we have:

$$\begin{aligned} \tau^{(s)} &= \sum_{i=0}^m b_{i,0}^{(s)} = \frac{b_{0,0}^{(s)}}{1-P_{eq}^{(s)}} = \frac{1-b_I^{(s)}}{\alpha^{(s)}(1-P_{eq}^{(s)})} = \\ &= \frac{2(1-b_I^{(s)})(1-2P_{eq}^{(s)})}{(W_0+1)(1-2P_{eq}^{(s)}) + W_0P_{eq}^{(s)}(1-(2P_{eq}^{(s)})^m)} \end{aligned} \quad (12)$$

whereby, we re-introduced the superscript (s) since this expression will be used in what follows.

The collision probability $P_{col}^{(s)}$ needed to compute $\tau^{(s)}$ can be found considering that using a 2-way hand-shaking mechanism, a packet from a transmitting station encounters a collision if in a given time slot, at least one of the remaining $(N-1)$ stations transmits one packet. Since each station has its own $\tau^{(s)}$, the collision probability for the s -th contending station depends on the transmission probabilities of the remaining stations as follows:

$$P_{col}^{(s)} = 1 - \prod_{\substack{j=1 \\ j \neq s}}^N (1 - \tau^{(j)}) \quad (13)$$

Given the set of N equations (1) and (12), a non-linear system of $2N$ equations can be solved in order to determine the values of $\tau^{(s)}$ and $P_{col}^{(s)}$ for any $s = 1, \dots, N$; this is the operating point corresponding to the N stations in the network needed in order to determine the aggregate throughput of the network, defined as the fraction of time the channel is used to successfully transmit payload bits:

$$S = \sum_{s=1}^N \frac{1}{T_{av}} P_s^{(s)} \cdot (1-P_e^{(s)}) \cdot PL \quad (14)$$

whereby, the summation is over the throughput related to the N contending stations, PL is the average payload size, and T_{av} is the expected time per slot defined in the following.

Probabilities involved in (14) are as follows: $P_e^{(s)}$ is the PER of the s -th station due to imperfect channel transmissions and

$P_s^{(s)}$ is the probability of successful packet transmission from the s -th station.

In the next section, we derive the mathematical relations defining both T_{av} and the probabilities involved in (14).

IV. ESTIMATING THE AVERAGE TIME SLOT DURATION

In order to proceed further, we need to evaluate the average time that a station spends in any possible state, i.e., the average time slot duration T_{av} , in terms of the key probabilities involved in the proposed model. This is the focus of the current section.

The average duration T_{av} of a time slot (or expected time per slot) can be evaluated by weighting the times spent by a station in a particular state with the probability of being in that state. It is possible to note four kinds of time slots.

- The average idle slot duration, identified by T_I , in which no station is transmitting over the channel.
- The average collision slot duration, identified by T_C , in which more than one station is attempting to gain access to the channel.
- The average duration of the slot due to erroneous transmissions because of imperfect channel conditions, identified by T_E .
- The average slot duration of a successful transmission, identified by T_S .

A. The average idle slot duration

The average idle slot duration can be evaluated as the probability $(1 - P_t)$ that no station is attempting to gain access to the channel times the duration σ of an empty slot time.

Let P_t be the probability that the channel is busy in a slot because at least one station is transmitting. Then, we have:

$$P_t = 1 - \prod_{s=1}^N (1 - \tau^{(s)}) \quad (15)$$

The average idle slot duration can be defined as:

$$T_I = P_I \cdot \sigma = (1 - P_t) \cdot \sigma \quad (16)$$

where each idle slot is assumed to have duration σ .

B. The average slot duration of a successful transmission

Consider a tagged station in the set of N stations in the analyzed network, and let s be its index in the set $\{1, \dots, N\}$. Then, the average slot duration of a successful transmission can be found upon evaluating the probability that only the s -th tagged station is successfully transmitting over the channel, i.e.,

$$P_s^{(s)} = \tau^{(s)} \prod_{\substack{j=1 \\ j \neq s}}^N (1 - \tau^{(j)}) \quad (17)$$

times the duration of a successful transmission from the s -th station, $T_s^{(s)}$. The latter depends on the rate-class (r) which the tagged station belong to, and can be evaluated as follows:

$$T_s^{(s)} = \frac{H_{PHY}}{R_C} + \frac{H_{MAC} + PL}{R_D^{(s)}} + \delta + \quad (18)$$

$$+ SIFS + \frac{H_{PHY} + ACK}{R_C} + \delta + DIFS$$

whereby, PL is the average payload length, H_{PHY} and H_{MAC} are, respectively, the physical and MAC header sizes, τ_p is the propagation delay, DIFS is the duration of the Distributed InterFrame Space, R_C is the basic data rate used for transmitting protocol data, and $R_D^{(s)}$ is the data rate of the s -th station.

With this setup, the average slot duration of a successful transmission can be evaluated as:

$$T_S = \sum_{i=1}^N P_s^{(i)} (1 - P_e^{(i)}) \cdot T_s^{(i)} \quad (19)$$

whereby, $(1 - P_e^{(i)})$ accounts for the probability of packet transmission without channel induced errors.

C. The average collision slot duration

In a network of stations transmitting equal length packets with different data rates, the average duration of T_C is largely dominated by the slowest transmitting stations. This phenomenon is called *performance anomaly* of 802.11b, and it has been first observed in [15].

As an example, suppose that a frame transmitted by a station using the rate 1 Mbps (class 1) collides with the one of a station transmitting at rate 11 Mbps one (class 4). Of course, both frames get corrupted while the channel appears busy to the remaining sensing stations for the whole duration of the frame transmitted by the low rate station. This implies that fast stations (high classes) are penalized by slow stations (low classes), causing a drop of the aggregate throughput. The duration of the collision depends on the frame duration of the lowest rate stations. In order to evaluate the collision probability, we define the class (r) collision duration as follows:

$$T_c^{(r)} = \frac{H_{PHY}}{R_C} + \frac{H_{MAC} + PL}{R_D^{(r)}} + ACK_{timeout} \quad (20)$$

which takes into account basic rate R_C and data rate $R_D^{(r)}$ of class (r).

For the derivations which follow, we consider a set of indexes which identify the stations transmitting with the r -th data rate:

$$n(r) = \{\text{identifiers of stations belonging to rate-class } (r)\}$$

$\forall r \in R = \{1, \dots, 4\}$ such that $\sum_{r=1}^N |n^{(r)}| = N$ ($|\cdot|$ is the cardinality of the embraced set).

With this setup, there are two different kinds of collisions:

- intra-class collisions between *at least* two frames belonging to same rate class (r);
- inter-class collisions between *at least* one frame of class (r) and *at least* one frame of class (j) $>$ (r)

As far as intra-class (r) collisions are concerned, the collision probability $P_{c1}^{(r)}$ can be evaluated as follows:

$$\left\{ 1 - \left[\prod_{s \in n(r)} (1 - \tau^{(s)}) + \sum_{s \in n(r)} \tau^{(s)} \prod_{\substack{j \in n(r) \\ j \neq s}} (1 - \tau^{(j)}) \right] \right\} \cdot \prod_{s \in \{S - n(r)\}} (1 - \tau^{(s)}) \quad (21)$$

Notice that the latter is the probability that stations not belonging to the same data rate set $n(r)$ do not transmit, times the probability that there are at least two stations in the same rate class $n(r)$ transmitting over the channel [17]. Notice that the first product within brace brackets accounts for the scenario in which no stations with rate in $n(r)$ transmit, or there is only one station transmitting with rate in $n(r)$. As a side note, notice that $P_{c1}^{(r)} = 0$ in case there are no collisions between stations belonging to the same rate class.

Following a similar reasoning, the inter-class (r) collision probability $P_{c2}^{(r)}$ can be evaluated as:

$$\left[1 - \prod_{s \in n(r)} (1 - \tau^{(s)}) \right] \cdot \left[1 - \prod_{j=r+1}^{N_R} \prod_{s \in n(j)} (1 - \tau^{(s)}) \right] \cdot \left[\prod_{j=1}^{r-1} \prod_{s \in n(j)} (1 - \tau^{(s)}) \right] \quad (22)$$

which considers the scenario in which at least one station of class (r) and at least one station belonging to a higher rate class (j) (i.e., ($j > r$)) transmit in the same time slot, while all the other stations belonging to lower indexed classes (i.e., with ($i < r$)) are silent. As a side note, notice that $P_{c2}^{(r)} = 0$ in case there are no collisions between stations belonging to different rate classes.

The total class (r) collision probability is the sum of the previous two probabilities:

$$P_c^{(r)} = P_{c1}^{(r)} + P_{c2}^{(r)} \quad (23)$$

while the average collision slot duration can be computed considering the whole set of classes $r \in R$ and their collision probabilities weighted by their durations:

$$T_C = \sum_{r=1}^{N_R} P_c^{(r)} \cdot T_c^{(r)} \quad (24)$$

D. The average duration of the slot due to erroneous transmissions

The average duration of the slot due to erroneous transmissions can be evaluated in a way similar to the one used for evaluating T_S and T_C :

$$T_E = \sum_{i=1}^N P_s^{(i)} \cdot P_e^{(i)} \cdot T_e^{(i)} \quad (25)$$

whereby, $P_s^{(i)}$ is defined in (17), and $T_e^{(s)}$ is assumed to be equal to $T_c^{(s)}$ since when a channel error occurs, the transmitting station does not receive the acknowledgment before the end of the ACK timeout.

E. Average time slot duration

Given the expected slots derived in the previous sections, the average duration of a slot time is simply:

$$T_{av} = T_I + T_C + T_S + T_E \quad (26)$$

V. TRAFFIC MODEL

This section presents the traffic model employed in our setup along with the derivation of the key probabilities $q^{(s)}$ and $P_{I,0}^{(s)}$ shown in Fig. 1. The offered load related to each station is characterized by the parameter $\lambda^{(s)}$ representing the rate at which packets arrive at the s -th station buffer from the upper layers, and measured in packets per second. The time between two packet arrivals is defined as *interarrival time*, and its mean value is evaluated as $\frac{1}{\lambda^{(s)}}$. One of the most commonly used traffic models assumes that the packet arrival process is Poisson. The resulting interarrival times are exponentially distributed.

In the proposed model shown in Fig. 1, we need to know the probability $q^{(s)}$ that there is at least one packet to be transmitted in the queue. Probability $q^{(s)}$ can be well approximated in a situation with small buffer size [11] through the following relation:

$$q^{(s)} = 1 - e^{-\lambda^{(s)} T_{av}} \quad (27)$$

where, T_{av} is the *expected time per slot*, which is useful to relate the state of the Markov chain with the actual time spent in each state. Such a time has been derived in (26). Under the hypothesis of small queue systems, probabilities $q^{(s)}$ and $P_{I,0}^{(s)}$ can be evaluated considering that the probability of having at least one packet arrival in the queue at the end of a successful packet transmission can be approximated with the probability of having at least one packet arrival in an average time slot duration. As a result of this simple approximation, we have $q^{(s)} = P_{I,0}^{(s)}$. Upon remembering (6) and (11), $\tau^{(s)}$ in (12) can be evaluated as:

$$\tau^{(s)} = \frac{q^{(s)} (1 - P_{eq}^{(s)})^{-1}}{q^{(s)} (\alpha^{(s)} - 1) + 1} = \frac{2(1 - 2P_{eq}^{(s)})q^{(s)}}{D(q^{(s)}, W_0, m, P_{eq}^{(s)})} \quad (28)$$

whereby,

$$D(q^{(s)}, W_0, m, P_{eq}^{(s)}) = q^{(s)} \left[(W_0 + 1)(1 - 2P_{eq}^{(s)}) + W_0 P_{eq}^{(s)} \cdot (1 - (2P_{eq}^{(s)})^m) \right] + 2(1 - q^{(s)})(1 - P_{eq}^{(s)})(1 - 2P_{eq}^{(s)}) \quad (29)$$

Though simple, this approximation has been verified by simulation, proving to be quite effective for predicting the aggregate throughput.

VI. PHYSICAL LAYER MODELING

In a scenario with N contending stations randomly distributed around a common access point, throughput performance depends on the channel conditions experienced by each station. In what follows we briefly recall the main signal propagation issues in order to evaluate the PER experienced by a generic station in the network. This will serve as the basis for the simulated scenarios discussed in Section VII.

A. Signal Propagation

Consider a contending station at distance d from an access point. Given the one-sided noise power spectral density³, N_o ,

³In what follows we will set the effective antenna temperature $T = 273K$ and $N_o = -174dBm$.

TABLE I
PHY SETUP OF THE IEEE 802.11B STANDARD.

Frequency [GHz]	2.4	2.4	2.4	2.4
Bit rate [Mbps]	1	2	5.5	11
Modulation	DBSPK	DQPSK	CCK	CCK
Chips per symbol, C_s	11	11	8	8
Bits per symbol, B_s	1	2	4	8
Channel band [MHz]	22	22	22	22
Minimum power of received signal (Sensitivity) [dBm]	-85	-82	-80	-76

TABLE III
TYPICAL NETWORK PARAMETERS

MAC header	28 bytes	Propag. delay τ_p	1 μs
PLCP Preamble	144 bit	PLCP Header	48 bit
PHY header	24 bytes	Slot time	20 μs
PLCP rate	1Mbps	W_0	32
No. back-off stages, m	5	W_{max}	1024
Payload size	1028 bytes	SIFS	10 μs
ACK	14 bytes	DIFS	50 μs
ACK timeout	364 μs	EIFS	364 μs

the received SNR can be evaluated as [23]:

$$SNR_{dB} = P(d) |_{dBm} - N_o - B_w |_{dB} - N_F \quad (30)$$

whereby, N_F is the receiver noise figure (10dB), while the power received at a distance d denoted $P(d) |_{dBm}$ is given by,

$$P(d) |_{dBm} = P_{tx} |_{dBm} - L(d) |_{dB} \quad (31)$$

In the previous equation, $L(d) |_{dB}$ is the path-loss at distance d from the transmitter

$$L(d) |_{dB} = L_o |_{dB} + 10 \cdot n_p \log_{10} \left(\frac{d}{d_0} \right)$$

and L_o is defined as,

$$L_o |_{dB} = -10 \log_{10} \left(\frac{G_t G_r \lambda^2}{(4\pi)^2 d_0^{n_p}} \right)$$

where, d_0 is a reference distance (usually selected equal to 1m) with path-loss L_o .

The other symbols are defined as follows; G_t is the transmitter antenna gain, G_r is the receiver antenna gain, n_p is the path-loss exponent, and $\lambda = c/f$ is the wavelength given by the ratio between the light velocity and the carrier frequency. The path-loss exponent n_p depends on the specific propagation environment and it ranges from 2 (free space propagation) to 3.5-4 for non-line-of-sight propagation, or multi-path fast fading conditions in indoor environments [23]. Furthermore, based on FCC regulations, in the 2.4GHz ISM band the transmitted power $P_{tx} |_{dBm}$ is 20dBm or equivalently, 100mW.

The SNR per transmitted bit γ accounts for the spreading gain C_s/B_s , and is defined as:

$$\gamma |_{dB} = SNR_{dB} + 10 \log_{10} \left(\frac{C_s}{B_s} \right) \quad (32)$$

whereby, C_s is the number of chips per symbol while B_s is the number of bits per transmitted symbol (see Table I).

B. IEEE 802.11b Physical Layer

The physical layer (PHY) of the basic 802.11b standard is based on the spread spectrum technology. Two options are specified, the Frequency Hopped Spread Spectrum (FHSS) and the Direct Sequence Spread Spectrum (DSSS). The FHSS uses Frequency Shift Keying (FSK) while the DSSS uses Differential Phase Shift Keying (DPSK) or Complementary Code Keying (CCK).

DSSS transmits signals in the 2.4-GHz ISM band (i.e., 2.4000-2.4835 GHz). The basic 802.11 DSSS gives data rates of 1 and 2 Mbps. The 802.11b extension [1] employs DSSS

at various rates including one employing CCK encoding on 4 and 8 bits for each CCK symbol, or optionally employing packet binary convolutional coding. The four supported data rates in 802.11b are 1, 2, 5.5 and 11 Mbps.

BER performance of the various transmitting modes of IEEE802.11b are shown in Table II for various channel models [2], [21], [22]. In Table II, the SNR in (32) is denoted as γ while $I_k(ab)$ is the modified Bessel function of k th order. The FER as a function of the SNR can be computed as follows:

$$P_e(\text{DATA}, \text{SNR}) = 1 - [1 - P_e(\text{PLCP}, \text{SNR})] \cdot [1 - P_e(\text{PSDU}, \text{SNR})] \quad (33)$$

where,

$$P_e(\text{PLCP}, \text{SNR}) = 1 - [1 - P_b(\text{DBPSK}, \text{SNR})]^{8 \times \text{PLCP}}, \quad (34)$$

and

$$P_e(\text{PSDU}, \text{SNR}) = 1 - [1 - P_b(\text{TYPE}, \text{SNR})]^{8 \times \text{PSDU}}. \quad (35)$$

In the previous equations, PLCP is the sum of the lengths of the PLCP Preamble and the PLCP header, PSDU is the sum of the lengths of the payload size PL and the MAC header and DATA = PSDU + PLCP.

$P_b(\text{DBPSK}, \text{SNR})$ is the BER as a function of SNR for the lowest data transmit rate employing DBPSK modulation (or DQPSK if the basic rate 2Mbps is adopted). Note that the FER, $P_e(\text{DATA}, \text{SNR})$, implicitly depends on the modulation format used. Hence, for each supported rate, one curve for $P_e(\text{DATA}, \text{SNR})$ as a function of SNR can be generated. $P_b(\text{TYPE}, \text{SNR})$ is modulation dependent whereby the parameter TYPE can be any of the following TYPE \in {DBPSK, DQPSK, CCK5.5, CCK11}⁴.

VII. SIMULATION RESULTS AND MODEL VALIDATION

This section focuses on simulation results for validating the theoretical models and derivations presented in the previous sections. We have developed a C++ simulator modeling both the DCF protocol details in 802.11b and the backoff procedures of a specific number of independent transmitting stations. The simulator considers an Infrastructure BSS (Basic Service Set) with an AP and a certain number of fixed stations which communicate only with the AP. For the sake of simplicity, inside each station there are only three fundamental working levels; traffic model generator, MAC and PHY layers. Traffic is generated following the exponential

⁴The acronyms are short for Differential Binary Phase Shift Keying, Differential Quadrature Phase Shift Keying and Complementary Code Keying with rate 5.5 or 11 Mbps, respectively.

TABLE II
BER $P_b(\gamma)$ FOR VARIOUS CHANNEL MODELS

Channel Model	DBPSK	DQPSK	CCK-5.5/11 Mbps
AWGN	$\frac{1}{2}\text{erfc}(\sqrt{\gamma})$	$Q_1(a, b) - \frac{1}{2}I_0(ab)e^{-\frac{1}{2}a^2 - \frac{1}{2}b^2}$ $a = \sqrt{2\gamma\left(1 - \sqrt{\frac{1}{2}}\right)}, b = \sqrt{2\gamma\left(1 + \sqrt{\frac{1}{2}}\right)}$ $Q_1(a, b) = e^{-\frac{a^2+b^2}{2}} \sum_{k=0}^{+\infty} \left(\frac{a}{b}\right)^k I_k(ab)$ $I_0(ab) = 1 + \sum_{k=1}^{+\infty} \left[\frac{(ab/2)^k}{k!}\right]^2$	$1 - \int_{-\sqrt{\gamma}}^{+\infty} \left[\int_{-(z+\sqrt{\gamma})}^{+(z+\sqrt{\gamma})} e^{-\frac{\eta^2}{2}} d\eta \right]^{\frac{\alpha-1}{2}} e^{-\frac{z^2}{2}} dz$ $\alpha = \begin{cases} 4, & 5.5 \text{ Mbps} \\ 8, & 11 \text{ Mbps} \end{cases}$
Rayleigh fading	$\frac{1}{2(1+\gamma)}$	$\frac{1}{2} \left[1 - \sqrt{\frac{\gamma\sqrt{2}}{1+\gamma\sqrt{2}}} \right]$	$\frac{2^{\alpha-1}}{2^{\alpha-1}} \sum_{i=1}^{\alpha-1} \frac{(-1)^{i+1} C_i^{\alpha-1}}{1+i+\gamma}$ $\alpha = \begin{cases} 4, & 5.5 \text{ Mbps} \\ 8, & 11 \text{ Mbps} \end{cases}$ $C_i^{\alpha-1} = \frac{(\alpha-1)!}{i!(\alpha-1-i)!}$

distribution for the packet interarrival times. Moreover, the MAC layer is managed by a state machine which follows the main directives specified in the standard [1], namely waiting times (DIFS, SIFS, EIFS), post-backoff, backoff, basic and RTS/CTS access modes. The typical MAC layer parameters for IEEE802.11b noted in Table III [1] have been used for performance validation.

For conciseness, in this paper we present a set of results related to the three scenarios described in the following.

The first investigated scenario considers $N = 10$ contending stations. Nine stations are randomly placed on the perimeter of a circle of radius R , while the AP is placed at the center of the transmission area. Upon employing equations (30)-(32) with $n_p = 4$ (typical of heavily faded Rayleigh channel conditions), we have chosen a distance $R = 20$ m in such a way that the SNR per transmitted bit is above the minimum sensitivity specified in Table I, relative to 11 Mbps bit rate. Such stations are in saturated conditions and have a packet rate $\lambda = 8$ kpkt/s. The payload size, assumed to be common to all the transmitting stations, is $PL = 1028$ bytes. The tenth station in the following is identified as the slow station and is placed at 4 different distances from the AP so that its transmission occurs with four different bit rates envisaged in the IEEE802.11b protocol.

The theoretical aggregate throughput achieved by the system in this scenario is depicted in Fig. 2 as a function of the packet rate of the slow station. Curves in both subplots have been parameterized with respect to the bit rate of the slow station. Simulated points are denoted with cross-points over the respective theoretical curves. The upper curves refer to ideal channel conditions, i.e., $\text{PER}=0$, while the lower subplot represents a scenario in which the packets transmitted by all the stations are affected by a PER equal to $8 \cdot 10^{-2}$, which is the worst-case situation with regards to the minimum sensitivity [1].

Some considerations are in order. Both subplots show that the aggregate throughput is significantly lower than 11 Mbps even though all the stations transmit at the highest bit rate (continuous curve). This is essentially due to overhead and control data transmitted at the basic rate R_C . Moreover,

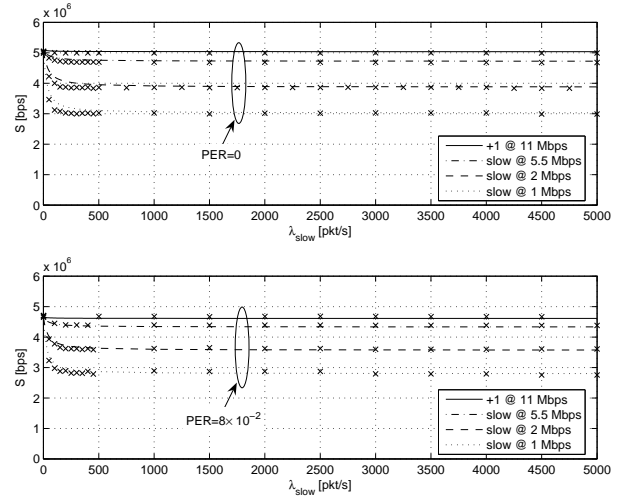


Fig. 2. Theoretical and simulated throughput for the 2-way mechanism as a function of the packet rate λ_{slow} of the slow station, for four different bit rates shown in the legends, and different PER values. Simulated points are identified by cross-markers over the respective theoretical curves. Payload size is 1028 bytes for all the $N = 10$ contending stations, whereby 9 stations are saturated and transmit with a packet rate of 8 kpkt/s at the maximum bit rate of 11 Mbps. In the upper subplot $\text{PER} = 0$, while in the lower one $\text{PER} = 8 \times 10^{-2}$.

throughput reduces as the PAR λ_{slow} increases, reaching saturation values strongly influenced by the rate of the slowest station. This phenomenon is called *performance anomaly* of 802.11b, and it has been first observed in [15]. A comparative analysis of the set of curves depicted in both subplots reveals that a small throughput reduction is due to the presence of channel induced errors.

The second investigated scenario is as follows. The four bit rates are equally distributed between 8 contending stations (2 stations with each bit rate). The packet rate λ is the same for all the contending stations and represents the independent variable against which the aggregate throughput in Fig. 3 is drawn. Curves have been parameterized with respect to the PER identified in the legends, assumed to be equal for all the contending stations. PER equal to zero represents ideal channel transmission conditions, while $\text{PER} = 8 \times 10^{-2}$ is the PER

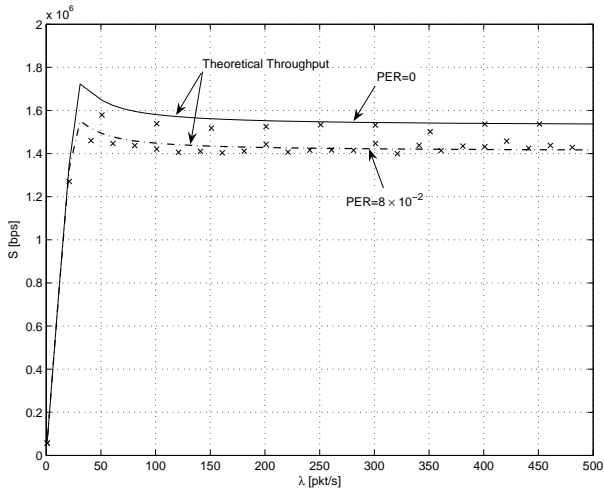


Fig. 3. Theoretical and simulated throughput for the 2-way mechanism as a function of the packet rate λ of the 8 contending stations, organized so that the four bit rates are equally distributed between the involved stations. Simulated points are identified by cross-markers over the respective theoretical curves. Payload size is $PL = 1028$ bytes for all the contending stations.

specified in the standard [1], corresponding to the minimum receiver sensitivity.

In addition to noting the expected throughput reduction due to the packet error rate, notice that the throughput manifests a linear behavior for low values of the packet rates with a slope depending mainly on the packet size of the contending stations. This observation will be further analyzed in the next section where a linear model for the throughput will be developed in unsaturated conditions. Moreover, note that in unsaturated traffic conditions, the aggregate throughput is quite independent of the packet errors due to non ideal channel conditions.

The last investigated scenario considers three saturated stations transmitting over a Rayleigh fading channel. Two stations transmit at the maximum bit rate of 11 Mbps, since they are located at 5 m distance from the AP. The third station is assumed to move radially from the AP, and to switch between the four envisaged bit rates as its distance from the AP increases. The aggregate throughput is shown in Fig. 4 as a function of the distance of the third station from the AP. While the theoretical throughput estimated with the proposed model is shown as a continuous curve, simulated results are noted with star-marked points. The radial distances from the AP at which rate switching occurs are noted with vertical lines in the same plot. Rate switching has been accomplished upon evaluating the minimum distance at which the per-station PER (according to the appropriate BER relation summarized in Table II along with expressions (33)-(35)) was above 8×10^{-2} for each employed bit rate, as specified in the standard [1], [2].

As already noted in the results presented in the previous plots, the aggregate throughput is strongly influenced by the bit rate of the slowest station. Up to about 26 m, the 3 stations transmit at the maximum bit rate and the aggregate throughput slightly decreases because of the worst BER conditions due to the SNR reduction of the moving station. As the distance increases and the bit rate of the moving stations decreases,

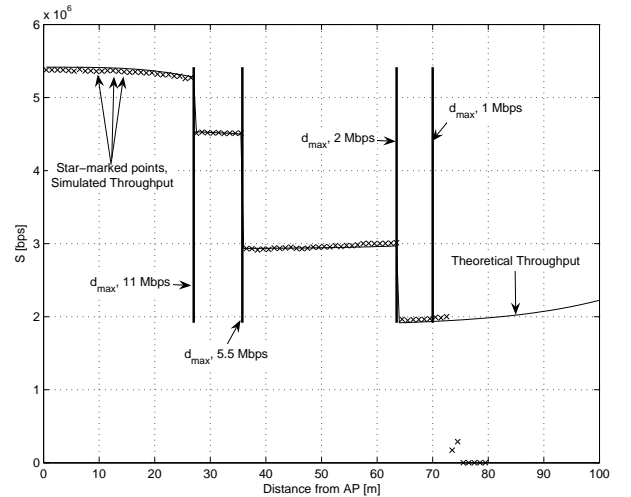


Fig. 4. Theoretical (continuous curve) and simulated (star-marked points) throughput for the 2-way mechanism for three saturated stations as a function of the distance from the AP of the third station. Payload size is $PL = 1028$ bytes for all the contending stations.

the behavior changes. In fact, at higher bit rates, the larger the distance, the more the moving station tends to go through backoff stages because of the increasingly worse channel conditions. The channel inactivity of the moving station is in favor of the other two fastest stations and the aggregate throughput tends to slightly increase.

VIII. A SIMPLE MODEL OF THE AGGREGATE THROUGHPUT IN NON-SATURATED CONDITIONS

This section derives a simple model of the aggregate throughput in unsaturated conditions. To this end, consider the aggregate throughput in (14)

$$S(\tau^{(1)}, \dots, \tau^{(N)}) = \sum_{s=1}^N \frac{1}{T_{av}} P_s^{(s)} \cdot (1 - P_e^{(s)}) \cdot PL \quad (36)$$

whereby, we have emphasized the dependence of $S(\tau^{(1)}, \dots, \tau^{(N)})$ on the set of N probabilities $\tau^{(1)}, \dots, \tau^{(N)}$, with $\tau^{(s)}$ defined in (12). Of course, probabilities $\tau^{(1)}, \dots, \tau^{(N)}$ depend on the traffic rates $\lambda^{(1)}, \dots, \lambda^{(N)}$ of the N contending stations as exemplified by (27) and (28).

Let us find an expression for $S(\tau^{(1)}, \dots, \tau^{(N)})$ when the overall system approaches unsaturated traffic conditions. In this respect, let us find the expressions for $P_s^{(s)}$, $P_e^{(s)}$ and T_{av} in the limit $\bar{\tau} \rightarrow \bar{0}$, whereby, the previous compact relation is used to signify the fact that all the probabilities $\tau^{(1)}, \dots, \tau^{(N)}$ approaches very small values.

First of all, notice that from (27) and (28), the following approximations easily follow:

$$\begin{aligned} q^{(s)} &\approx \lambda^{(s)} T_{av}, & \lambda^{(s)} &\rightarrow 0, \forall s = 1, \dots, N \\ \tau^{(s)} &\approx \frac{\lambda^{(s)} T_{av}}{1 - P_{eq}^{(s)}}, & \lambda^{(s)} &\rightarrow 0, \forall s = 1, \dots, N \end{aligned} \quad (37)$$

From (13), it easily follows

$$\lim_{\bar{\tau} \rightarrow \bar{0}} P_{col}^{(s)} = 0, \forall s = 1, \dots, N$$

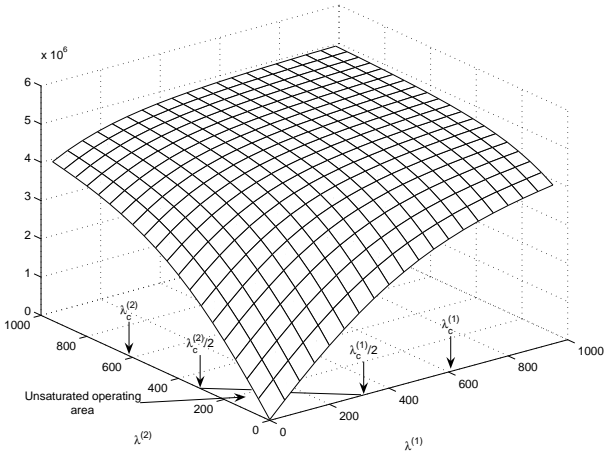


Fig. 5. Aggregate throughput for $N = 2$, 11Mbps contending stations over the bi-dimensional set $\lambda^{(1)} \in [0, 1000]$ pkt/s, $\lambda^{(2)} \in [0, 1000]$ pkt/s, for $PL = 1028$ bytes. The other transmission parameters are noted in Table III.

Given the relation $P_{eq}^{(s)} = P_e^{(s)} + P_{col}^{(s)} - P_e^{(s)}P_{col}^{(s)}$ in (1), as $\bar{\lambda} \rightarrow \bar{0}$ (which is tantamount to considering $\bar{\tau} \rightarrow \bar{0}$ in light of the relation (37)) we have:

$$P_{eq}^{(s)} \rightarrow P_e^{(s)}, \quad \forall s = 1, \dots, N$$

From (17), as $\bar{\tau} \rightarrow \bar{0}$ the following relation holds,

$$P_s^{(s)} \approx \tau^{(s)} \approx \frac{\lambda^{(s)} T_{av}}{1 - P_e^{(s)}}, \quad \forall s = 1, \dots, N$$

Upon employing the previous relations, (36) can be rewritten as:

$$S(\lambda^{(1)}, \dots, \lambda^{(N)}) \approx PL \cdot \sum_{s=1}^N \lambda^{(s)} \quad (38)$$

which is valid under the hypothesis that the packet length PL is the same for all the N contending stations. In case of different packet lengths, the aggregate throughput is the weighted sum of each station packet rate times the respective packet length.

Notice that in unsaturated conditions, the aggregate throughput is independent from the packet error rate affecting data transmission from each contending station in the network.

Equ. (38) states that for very low values of $\lambda^{(s)}$, $\forall s = 1, \dots, N$, the aggregate throughput behaves as a linear combination of the packet rates of the N contending stations times the average payload length PL . As a reference example, consider the aggregate throughput⁵ shown in Fig. 5 for a scenario with $N = 2$ (11Mbps) contending stations. In this reference example, we have considered ideal channel conditions (i.e., $P_e^{(s)} = 0$, $\forall s = 1, 2$) so that only collisions can yield packet losses. The other transmission parameters are noted in Table III. There are various points that are worth noting from this figure. When both stations approach saturated conditions, i.e., for $\lambda^{(1)}$ and $\lambda^{(2)}$ tending to infinity, the maximum aggregate throughput is less than half the maximum bit rate of each contending station due to overhead and control

⁵The throughput has been plotted using (14) evaluated by employing the solution of the non-linear system of $2N$ equations discussed at the end of Section III.

data transmitted at the basic rate R_C . On the other hand, when both $\lambda^{(1)}$ and $\lambda^{(2)}$ take on very small values, the aggregate throughput points define a plane predicted by (38) in the region $(\lambda^{(1)}, \lambda^{(2)}) \in D_2$ defined as follows

$$D_2 = \left\{ \begin{array}{l} \lambda^{(1)} \in \left[0, \frac{\lambda_c^{(1)}}{2}\right) \\ 0 \leq \lambda^{(2)} \leq -\frac{\lambda_c^{(2)}}{\lambda_c^{(1)}} \lambda^{(1)} + \frac{\lambda_c^{(2)}}{2} \end{array} \right. \quad (39)$$

whereby, $\lambda_c^{(1)}$ and $\lambda_c^{(2)}$ marked on Fig. 5, represents the limiting values of the packet rate above which each station approaches saturated traffic conditions⁶. Region D_2 along with the line⁷ $\lambda^{(2)} = -\frac{\lambda_c^{(2)}}{\lambda_c^{(1)}} \lambda^{(1)} + \frac{\lambda_c^{(2)}}{2}$ is identified as *unsaturated operating area* in Fig. 5.

Consider now the previous scenario with two 11Mbps contending stations transmitting at a fixed packet rate $\lambda^{(1)} = \lambda^{(2)} = 50$ pkt/s (unsaturated conditions for both stations), and a third station starts transmitting at a bit rate equal to 1 Mbps. As above, we have considered ideal channel conditions for the two 11 Mbps stations (i.e., $P_e^{(s)} = 0$, $\forall s = 1, 2$) while the third station is assumed to experience three different PER values $P_e^{(3)} = 0, 10^{-1}, 10^{-2}$.

Fig. 6 shows the aggregate throughput as a function of the packet rate $\lambda^{(3)}$ of the third station. It can be observed that when $\lambda^{(3)}$ takes on low values, the overall system can be considered in unsaturated conditions, and therefore model (38) holds. In this case, $S(\lambda^{(1)}, \lambda^{(2)}, \lambda^{(3)})$ can be considered as a line with slope equal to the average packet length PL , while $PL(\lambda^{(1)} + \lambda^{(2)}) = PL \cdot 100$ pkt/s is the value of $S(\lambda^{(1)}, \lambda^{(2)}, \lambda^{(3)})$ for $\lambda^{(3)} = 0$. So long as $\lambda^{(3)} \in [0, \lambda_c^{(3)}/2]$, model (38) predicts the aggregate throughput quite well without the necessity of solving the non-linear system described at the end of Section III. On the other hand, when $\lambda^{(3)}$ grows above $\lambda_c^{(3)}/2$, the system approaches saturated conditions quite fast and the overall throughput drops asymptotically to 1.3Mbps, as shown in Fig. 6 for $\lambda^{(3)} \rightarrow \infty$. Notice that the aggregate throughput is strongly influenced by that of the slowest contending station (1 Mbps in this specific case), confirming the rate anomaly problem already noted in literature by resorting to simulations [15]. Also note that the PER experienced by the third station as already demonstrated theoretically above, does not affect the linear zone of the aggregate throughput, while it reduces the aggregate throughput obtained in saturated conditions. Also shown in the same figure is the throughput of the third station (when the first two stations are silent, i.e., $\lambda^{(1)} = \lambda^{(2)} = 0$ pkt/s) along with the linear model of the throughput valid for values of $\lambda^{(3)}$ lower than $\lambda_c^{(3)}$.

For N contending stations, the region D_N is the volume

⁶For the considerations that follow, let us suppose the values of $\lambda_c^{(1)}$ and $\lambda_c^{(2)}$ are known. Their values will actually be derived later.

⁷This is the equation of the line passing through the two points $(0, \lambda_c^{(2)}/2)$ and $(\lambda_c^{(1)}/2, 0)$.

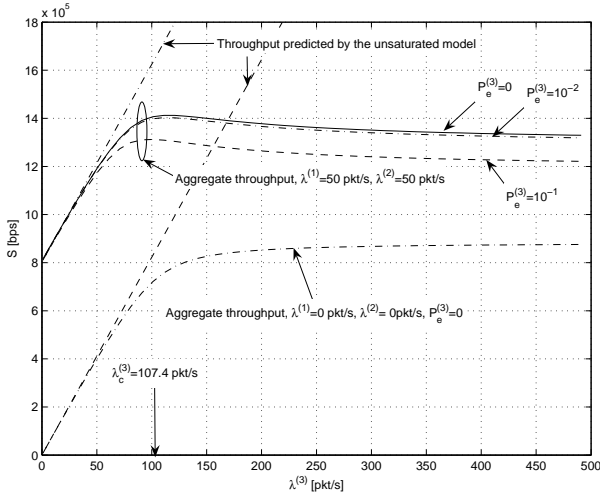


Fig. 6. Theoretical and Simulated Throughput for a scenario with three contending stations with the following transmission parameters: the first two stations transmit with a bit rate of 11Mbps, while the third one is a 1Mbps station. Payload size is 1028 bytes for all stations. Packet rates are noted in the figure for the two scenarios investigated. Dash-dotted line refers to the linear model of the throughput derived in (38).

contained in the region $(\lambda^{(1)}, \dots, \lambda^{(N)}) \in D_N$ defined as

$$D_N = \begin{cases} \lambda^{(1)} \in \left[0, \frac{\lambda_c^{(1)}}{2}\right) \\ \dots \\ \lambda^{(N-1)} \in \left[0, \frac{\lambda_c^{(N-1)}}{2}\right) \\ 0 \leq \lambda^{(N)} \leq \frac{\lambda_c^{(N)}}{2} - \lambda_c^{(N)} \sum_{s=1}^{N-1} \frac{\lambda^{(s)}}{\lambda_c^{(s)}} \end{cases} \quad (40)$$

whereby, the last equation is the hyperplane passing through the N -dimensional points

$$\left(\frac{\lambda_c^{(1)}}{2}, 0, \dots, 0\right), \left(0, \frac{\lambda_c^{(2)}}{2}, \dots, 0\right), \dots, \left(0, \dots, 0, \frac{\lambda_c^{(N)}}{2}\right)$$

The natural question at this point is the determination of the critical packet rates $\lambda_c^{(s)}$, $\forall s = 1, \dots, N$, needed in order to identify the interval of validity of the aggregate throughput in (38). Consider the s -th station in the network. Such a station is in saturation when there is always a packet to be transmitted in its buffer. A simple threshold on $\lambda^{(s)}$ discerning unsaturated from saturated operation is $\lambda_c^{(s)} = \frac{1}{T_{st}}$, whereby T_{st} is the service time of the s -th station. The reason is simple; the service time is the time interval from when a packet is taken from the queue head, to when it is successfully transmitted. If the packet inter-arrival time in the buffer is greater than T_{st} , then on the average, the buffer will contain at most one packet waiting for transmission. On the other hand, when the packet inter-arrival time is less than T_{st} , then packets will be buffered for successive transmissions. In this respect, T_{st} is the equilibrium interval based on which on average a packet is transmitted soon after its arrival in the buffer.

The service time T_{st} can be defined as follows [10], [19]:

$$T_{st} = T_A + T_{TX}$$

whereby, T_A is the average time that a station spends through the various backoff stages before transmitting a packet, i.e., the so called MAC access time, while T_{TX} is the average duration of a transmission.

TABLE IV
CRITICAL PACKET RATES.

Station bit rate	1 Mbps	2 Mbps	5.5 Mbps	11 Mbps
$\lambda_c^{(r)}$ -[pkt/s]	107.4	196.5	416.3	612.0

As far as T_A is concerned, we note that despite the existence of $m + 1$ backoff stages (see Fig. 1), in unsaturated conditions where the collisions between stations rarely occur, a packet is transmitted in the 0-th backoff stage after an average number of backoff slots equal to $W_0/2$. Based on these considerations, the average MAC access time in unloaded traffic conditions can be simply defined as

$$T_A = \frac{W_0}{2} \sigma \quad (41)$$

whereby, σ is the duration of an empty slot.

The average duration of a transmission, T_{TX} , can be evaluated by observing that a station can experience two possible situations; successful transmission or collision. Upon neglecting the effects of collisions based on the considerations stated above in connection to T_A , T_{TX} can be defined as in (18); $T_{TX} = T_s^{(s)}$.

The values of $\lambda_c^{(r)}$ derived under these hypotheses, are shown in Table IV as a function of the station transmission bit rate.

IX. CONCLUSIONS

In this paper, we have presented a multi-dimensional Markovian state transition model characterizing the DCF behavior at the MAC layer of the IEEE802.11 series of standards by accounting for channel induced errors and multirate transmission typical of fading environments, under both non-saturated and saturated traffic conditions. The model provided in the paper allows taking into consideration the impact of channel contention in throughput analysis which is often not considered or is considered with a static model by using a mean contention period. Subsequently, based on justifiable assumptions, the stationary probability of the Markov chain is calculated obtaining the throughput in both non-saturated and saturated conditions.

Finally, we have shown that the behavior of the aggregate throughput in non-saturated traffic conditions is a linear combination of the payload size along with the packet rates of each contending station in the network. This result is significant for system level optimization of the network. Theoretical derivations were supported by simulations.

REFERENCES

- [1] *IEEE Standard for Wireless LAN Medium Access Control (MAC) and Physical Layer (PHY) Specifications*, November 1997, P802.11
- [2] *IEEE Std 802.15.2-2003; Part 15.2: Coexistence of Wireless Personal Area Networks with Other Wireless Devices Operating in Unlicensed Frequency Bands*, August 2003.
- [3] G. Bianchi, "Performance analysis of the IEEE 802.11 distributed coordination function", *IEEE JSAC*, Vol.18, No.3, March 2000.
- [4] Ha Cheol Lee, "Impact of bit errors on the DCF throughput in wireless LAN over rician fading channels", *In Proc. of IEEE ICDDT '06*, 2006.

- [5] Q. Ni, T. Li, T. Turletti, and Y. Xiao, "Saturation throughput analysis of error-prone 802.11 wireless networks", *Wiley Journal of Wireless Communications and Mobile Computing*, Vol. 5, No. 8, pp. 945-956, Dec. 2005.
- [6] P. Chatzimisios, A.C. Boucouvalas, and V. Vitsas, "Influence of channel BER on IEEE 802.11 DCF", *IEE Electronics Letters*, Vol.39, No.23, pp.1687-1689, Nov. 2003.
- [7] M. Zorzi and R.R. Rao, "Capture and retransmission control in mobile radio", *IEEE JSAC*, Vol.12, No.8, pp.1289 - 1298, Oct. 1994.
- [8] Jae Hyun Kim and Jong Kyu Lee "Capture effects of wireless CSMA/CA protocols in Rayleigh and shadow fading channels", *IEEE Trans. on Veh. Tech.*, Vol.48, No.4, pp.1277-1286, July 1999.
- [9] Z. Hadzi-Velkov and B. Spasenovski, "Capture effect in IEEE 802.11 basic service area under influence of Rayleigh fading and near/far effect", *In Proc. of 13th IEEE International Symposium on Personal, Indoor and Mobile Radio Communications*, Vol.1, pp.172 - 176, Sept. 2002.
- [10] L. Yong Shyang, A. Dadej, and A.Jayasuriya, "Performance analysis of IEEE 802.11 DCF under limited load", *In Proc. of Asia-Pacific Conference on Communications*, Vol.1, pp.759 - 763, 03-05 Oct. 2005.
- [11] D. Malone, K. Duffy, and D.J. Leith, "Modeling the 802.11 distributed coordination function in non-saturated heterogeneous conditions", *IEEE-ACM Trans. on Networking*, vol. 15, No. 1, pp. 159172, Feb. 2007.
- [12] F. Daneshgaran, M. Laddomada, F. Mesiti, and M. Mondin, "Unsaturated Throughput Analysis of IEEE 802.11 in Presence of Non Ideal Transmission Channel and Capture Effects," *to appear on IEEE Trans. on Wireless Communications*, 2008.
- [13] F. Daneshgaran, M. Laddomada, F. Mesiti, and M. Mondin, "A Model of the IEEE 802.11 DCF in presence of non ideal transmission channel and capture effects," *In Proc. of IEEE Globecom 07*, Washington DC, November 2007.
- [14] D. Qiao, S. Choi, and K.G. Shin, "Goodput analysis and link adaptation for IEEE 802.11a wireless LANs", *IEEE Trans. On Mobile Computing*, Vol.1, No.4, Oct.-Dec. 2002.
- [15] Heusse M.,Rousseau F., Berger-Sabbatel G. and Duda A., "Performance anomaly of 802.11b" *In Proc. of IEEE INFOCOM 2003*, pp. 836-843.
- [16] T. Joshi, A. Mukherjee, and D.P. Agrawal, "Analytical modeling of the link delay characteristics for IEEE 802.11 DCF multi-rate WLANs," *In Proc. of IEEE CCECE-CCGEL*, pp. 2164-2167, May 2006.
- [17] D.-Y. Yang, T.-J. Lee, K. Jang, J.-B. Chang, and S. Choi, "Performance enhancement of multirate IEEE 802.11 WLANs with geographically scattered stations," *IEEE Trans. on Mobile Computing*, vol.5, no.7, pp.906-919, July 2006.
- [18] G.R. Cantieni, Q. Ni, C. Barakat, and T. Turletti, "Performance analysis under finite load and improvements for multirate 802.11," *Computer Communications*, Elsevier, vol.28, pp.1095-1109, 2005.
- [19] W. Lee, C. Wang, and K. Sohrawy, "On use of traditional M/G/1 model for IEEE 802.11 DCF in unsaturated traffic conditions", *In Proc. of IEEE WCNC*, 2006, pp. 19331937.
- [20] G. Bolch, S. Greiner, H. de Meer, and K.S. Trivedi, *Queueing Networks and Markov Chains*, Wiley-Interscience, 2nd edition, 2006.
- [21] M.K. Simon and M. Alouini, *Digital Communication over Fading Channels: A Unified Approach to Performance Analysis*, Wiley-Interscience, 1st edition, 2000.
- [22] M. Fainberg, *A Performance analysis of the IEEE 802.11b local area network in the presence of bluetooth personal area network*, Available at <http://eeweb.poly.edu/dgoodman/fainberg.pdf>.
- [23] T. S. Rappaport, *Wireless Communications, Principles and Practice*, Prentice-Hall, 2nd edition, USA, 2002.
- [24] Wu Xiuchao, "Simulate 802.11b Channel within NS-2", available online at http://www.comp.nus.edu.sg/~wuxiucha/research/reactive/report/80211ChannelinNS2_new.pdf

